

UHE neutrinos from superconducting cosmic strings

Veniamin Berezhinsky,^{1,*} Ken D. Olum,^{2,†} Eray Sabancilar,^{2,‡} and Alexander Vilenkin^{2,§}

¹*INFN, Laboratori Nazionali del Gran Sasso, I-67010 Assergi (AQ), Italy*

²*Institute of Cosmology, Department of Physics and Astronomy,
Tufts University, Medford, MA 02155, USA.*

Abstract

Superconducting cosmic strings naturally emit highly boosted charge carriers from cusps. This occurs when a cosmic string or a loop moves through a magnetic field and develops an electric current. The charge carriers and the products of their decay, including protons, photons and neutrinos, are emitted as narrow jets with opening angle $\theta \sim 1/\gamma_c$, where γ_c is the Lorentz factor of the cusp. The excitation of electric currents in strings occurs mostly in clusters of galaxies, which are characterized by magnetic fields $B \sim 10^{-6}$ G and a filling factor $f_B \sim 10^{-3}$.

Two string parameters determine the emission of the particles: the symmetry breaking scale η , which for successful applications should be of order 10^9 – 10^{12} GeV, and the dimensionless parameter i_c , which determines the maximum induced current as $J_{\max} = i_c e \eta$ and the energy of emitted charge carriers as $\epsilon_X \sim i_c \gamma_c \eta$, where e is the electric charge of a particle. For the parameters η and B mentioned above, the Lorentz factor reaches $\gamma_c \sim 10^{12}$ and the maximum particle energy can be as high as $\gamma_c \eta \sim 10^{22}$ GeV. The diffuse fluxes of UHE neutrinos are close to the cascade upper limit, and can be detected by future neutrino observatories. The signatures of this model are: very high energies of neutrinos, in excess of 10^{20} eV, correlation of neutrinos with clusters of galaxies, simultaneous appearance of several neutrino-produced showers in the field of view of very large detectors, such as JEM-EUSO, and 10 TeV gamma radiation from the Virgo cluster. The flux of UHE protons from cusps may account for a large fraction of the observed events at the highest energies.

PACS numbers: 98.70.Sa 98.80.Cq 11.27.+d

*Electronic address: venya.berezhinsky@lngs.infn.it

†Electronic address: kdo@cosmos.phy.tufts.edu

‡Electronic address: eray.sabancilar@tufts.edu

§Electronic address: vilenkin@cosmos.phy.tufts.edu

I. INTRODUCTION

A. Neutrino astronomy

Ultra-high-energy (UHE) neutrino astronomy at energies above 10^{17} eV is based on new, very efficient methods of neutrino detection and on exciting theories for neutrino production. The most interesting range of this astronomy covers tremendously high energies above $10^{19} - 10^{20}$ eV. In fact, this energy scale gives only the low-energy threshold, where the new observational methods, such as space-based observations of fluorescent light and radio and acoustic methods, start to operate. These methods allow observation of very large areas and so detection of tiny fluxes of neutrinos. For example the exposure of the space detector JEM-EUSO [1] is planned to reach $\sim 10^6$ km²yr sr. The upper limits obtained by radio observations are presented in Fig. 1.

The basic idea of detection by EUSO is similar to the fluorescence technique for observations of extensive air showers (EAS) from the surface of the Earth. The UHE neutrino entering the Earth's atmosphere produces an EAS. A known fraction of its energy, which reaches 90%, is radiated in the form of isotropic fluorescent light, which can be detected by an optical telescope in space. There is little absorption of up-going photons, so the fraction of flux detected is known, and thus EUSO provides a calorimetric measurement of the primary energy. In the JEM-EUSO project [1] a telescope with diameter 2.5 m will observe an area $\sim 10^5$ km² and will have a threshold for EAS detection $E_{\text{th}} \sim 1 \times 10^{19}$ eV. The observations are planned to start in 2012–2013.

UHE neutrinos may also be very efficiently detected by observations of radio emission by neutrino-induced showers in ice or lunar regolith. This method was originally suggested by G. Askaryan in the 1960s [2]. Propagating in matter the shower acquires excess negative electric charge due to scattering of the matter electrons. The coherent Cerenkov radiation of these electrons produces a radio pulse. Recently this method has been confirmed by laboratory measurements [3]. Experiments have searched for such radiation from neutrino-induced showers in the Greenland and Antarctic ice and in the lunar regolith. In all cases the radio emission can be observed only for neutrinos of extremely high energies. Upper limits on the flux of these neutrinos have been obtained in the GLUE experiment [4] by radiation from the moon, in the FORTE experiment [5] by radiation from the Greenland ice, and in the ANITA [6] and RICE [7] experiments from the Antarctic ice.

Probably the first proposal for detection of UHE neutrinos with energies higher than 10^{17} eV was made in [8]. It was proposed there to use the horizontal Extensive Air Showers (EAS) for neutrino detection. Later this idea was transformed into the Earth-skimming effect [9] for τ neutrinos. Recently the Auger detector [10] put an upper limit on UHE neutrino flux using the Earth-skimming effect (see Fig. 1).

B. UHE neutrino sources

What might these new large-area UHE neutrino observatories detect? On the one hand, there are without doubt *cosmogenic neutrinos*, produced by UHECR particles interacting with the CMB photons. On the other hand, there may be neutrinos produced in decays or annihilation of superheavy particles; this is referred to as the *top-down scenario*.

Cosmogenic neutrinos were first discussed in [11], soon after the prediction of the GZK cutoff [12]. There, it was shown that UHE neutrino fluxes much higher than the observed

UHECR flux can be produced by protons interacting with CMB photons at large redshifts. The predicted flux depends on the cosmological evolution of the sources of UHE protons and on the assumed acceleration mechanisms. Recent calculations of cosmogenic neutrino fluxes (see e.g. [13]–[20]) are normalized to the observed UHECR flux, with different assumptions about the sources.

The energies of cosmogenic neutrinos are limited by the maximum energy of acceleration, $E_{\text{acc}}^{\text{max}}$. To provide neutrinos with energies above 1×10^{20} eV, the energies of accelerated protons must exceed 2×10^{21} eV. For non-relativistic shocks, the maximum energy of acceleration E_p^{max} can optimistically reach 1×10^{21} eV. For relativistic shocks this energy can be somewhat higher. Production of cosmogenic neutrinos with still higher energies depends on less-developed ideas, such as acceleration in strong electromagnetic waves, exotic plasma mechanisms of acceleration and unipolar induction.

The top-down scenarios, on the other hand, naturally provide neutrinos with energies higher and much higher than 1×10^{20} eV [21]. The mechanism common to many models assumes the existence of superheavy particles with very large masses up to the GUT scale $\sim 10^{16}$ GeV. Such particles can be produced by Topological Defects (TD) (see [22] for a general review). They then rapidly decay and produce a parton cascade, which is terminated by production of pions and other hadrons. Neutrinos are produced in hadron decays.

The production of unstable superheavy particles — the constituent fields of TD — is a very common feature of the TD [23]. However, the dynamics of TD is highly nonlinear and complicated, the distance between TDs is model-dependent, and the calculation of UHE particle fluxes requires special consideration for different types of TD [24].

Cosmic strings can release particles in the process of self-interaction, and in the final evaporation of tiny loops, but only a few particles are produced by each such interaction. Of more interest are cosmic string *cusps*, where the string doubles back on itself and moves with a huge Lorentz factor [25]. Particles emitted by cusps have energies much higher than their rest masses, because of the boost. However, the flux from such events is too low to be observed [26, 27].

Monopole-antimonopole pairs connected by strings [28–30] can release superheavy particles when the monopole and antimonopole finally annihilate. However, such defects, similar to superheavy dark matter (see below), would be accumulated inside galaxies, and in particular in the Milky Way. The resulting UHECR flux would be dominated by photons, which can reach us easily from short distances. Such photons are not observed [31] at the level that would be necessary if top-down production were to account for the observed UHECR.

If each monopole is attached to two strings, we have *necklaces*. Necklaces are an attractive source for UHE neutrinos [32, 33], but simple models of necklaces may lead to rapid annihilation of the monopoles [34]. In other models, however, the monopoles may survive for much longer, providing a detectable flux of UHE neutrinos.¹

In a wide class of particle physics models, cosmic strings can be *superconducting*, in which case they respond to external electromagnetic fields as thin superconducting wires [35]. String superconductivity arises when a condensate of charged particles (which can be

¹ The main point of Ref. [34] is that the relativistic motion of strings causes monopoles to develop large velocities along the string. As a result monopoles frequently run into one another and annihilate. A possible way to avoid this is to consider light strings, which remain overdamped till very late times and therefore move slowly. Another possibility is that the strings have zero modes, which act as a one-dimensional gas on the strings and slow the monopoles down. These models need further investigation.

either bosons or fermions) is bound to the string. These particles have zero mass in the bound state, whereas away from the string they have some mass m_X . Loops of superconducting string develop electric currents as they oscillate in cosmic magnetic fields. Near a cusp, a section of string acquires a large Lorentz boost γ_c , and simultaneously the string current is increased by a factor γ_c . If the current grows to a critical value J_{max} charge carriers rapidly scatter off each other and are ejected from the string. The decay products of these particles can then be observed as cosmic rays. This model will be the subject of the present paper.

Apart from TDs, superheavy particles can naturally be produced by thermal processes [36, 37] and by time-varying gravitational fields [38, 39] shortly after the end of inflation. These particles can survive until present and produce neutrinos in their decays. Protected by symmetry (e.g. discrete gauge symmetry, in particular R-parity in supersymmetric theories), these particles can have very long lifetimes exceeding the age of the universe. The resulting neutrino flux may exceed the observed flux of UHECR. However, like any other form of CDM, superheavy particles accumulate in the Milky Way halo and produce a large flux of UHE photons. The non-observation of these photons puts an upper limit on the neutrino flux from intergalactic space.

C. The cascade bound

The neutrino fluxes are limited from above. The most general upper bound for UHE neutrinos, valid for both cosmogenic neutrinos and neutrinos from top-down models, is given by the *cascade upper limit*, first considered in [8, 40]. The production of neutrinos in these scenarios is accompanied by production of high energy photons and electrons. Colliding with low-energy target photons, a primary photon or electron produces an electromagnetic cascade due to the reactions $\gamma + \gamma_{\text{target}} \rightarrow e^+ + e^-$, $e + \gamma_{\text{target}} \rightarrow e' + \gamma'$, etc. The cascade spectrum is very close to the EGRET observations in the range 3 MeV - 100 GeV [41]. The observed energy density in this range is $\omega_{\text{EGRET}} \approx (2-3) \times 10^{-6}$ eV/cm³. To be conservative, we will use the lower end of this range. It provides the upper limit for the cascade energy density. The upper limit on UHE neutrino flux $J_\nu(> E)$ (sum of all flavors) is given by the following chain of inequalities

$$\omega_{\text{cas}} > \frac{4\pi}{c} \int_E^\infty E' J_\nu(E') dE' > \frac{4\pi}{c} E \int_E^\infty J_\nu(E') dE' \equiv \frac{4\pi}{c} E J_\nu(> E). \quad (1)$$

Here c is the speed of light, but will generally work in units where $c = 1$ and $\hbar = 1$. In terms of the differential neutrino spectrum, Eq. (1) gives $J_\nu(E)$ gives

$$E^2 J_\nu(E) < \frac{c}{4\pi} \omega_{\text{cas}}, \quad \text{with } \omega_{\text{cas}} < \omega_{\text{EGRET}} \quad (2)$$

Eq. (2) gives a *rigorous* upper limit on the neutrino flux. It is valid for neutrinos produced by HE protons, by topological defects, by annihilation and decays of superheavy particles, i. e., in all cases when neutrinos are produced through decay of pions and kaons. It holds for an arbitrary neutrino spectrum decreasing with energy. If one assumes some specific shape of neutrino spectrum, the cascade limit becomes stronger. For a generation spectrum proportional to E^{-2} , which is used for analysis of observational data, one obtains a stronger upper limit. Given for one neutrino flavor it reads [42]

$$E^2 J_i(E) \leq \frac{1}{3} \frac{c}{4\pi} \frac{\omega_{\text{cas}}}{\ln(E_{\text{max}}/E_{\text{min}})}, \quad (3)$$

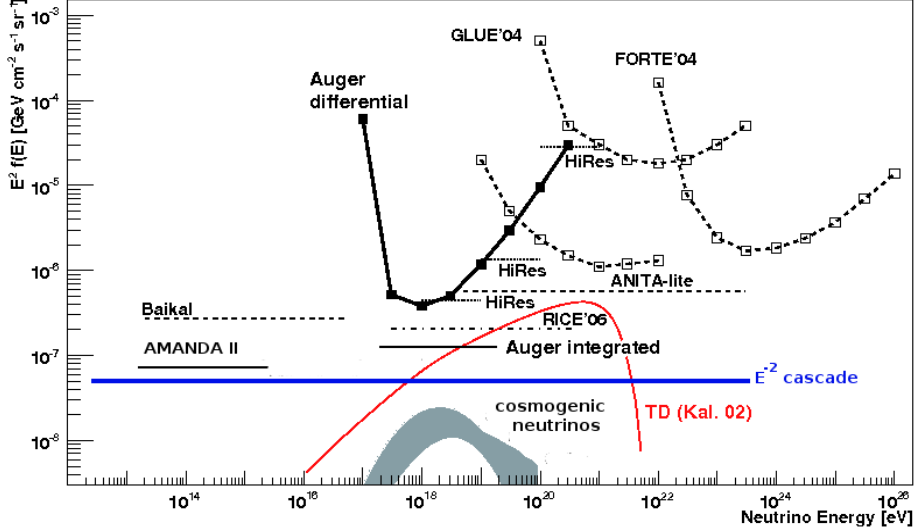


FIG. 1: The experimental upper limits on UHE neutrino fluxes in comparison with the electromagnetic cascade upper limit in assumption of E^{-2} generation spectrum (labeled “ E^{-2} cascade”) and with predictions for cosmogenic neutrinos. Neutrino fluxes are given for one neutrino flavor $\nu_i + \bar{\nu}_i$.

where E_{\max} and E_{\min} give the range of neutrino energies to which the E^{-2} spectrum extends, and $i = \nu_\mu + \bar{\nu}_\mu$, or $i = \nu_e + \bar{\nu}_e$, or $i = \nu_\tau + \bar{\nu}_\tau$. This upper limit is shown in Fig. 1. One can see that the observations almost reach the cascade upper limit and thus almost enter the region of allowed fluxes.

The most interesting energy range in Fig. 1 corresponds to $E_\nu > 10^{21}$ eV, where acceleration cannot provide protons with sufficient energy for production of these neutrinos. At present the region of $E_\nu > 10^{21}$ eV, and especially $E_\nu \gg 10^{21}$ eV is considered as a signature of top-down models, which provide these energies quite naturally.

D. Model assumptions

In this paper we consider superconducting string loops as a source of UHE neutrinos. We consider a simple model in which a magnetic field of magnitude B , occupying a fraction of space f_B , is generated at some epoch $z_{\max} \sim 2-3$. The strings are characterized by two parameters: the fundamental symmetry breaking scale η and the critical current J_{\max} . We take the mass per unit length of string to be $\mu = \eta^2$.

The predicted flux of UHE neutrinos depends on the typical length of loops produced by the string network. This issue has been a subject of much recent debate, with different simulations [43–46] and analytic studies [47, 48] yielding different answers. Here we shall adopt the picture suggested by the largest and, in our view, the most accurate simulations of string evolution performed to date [45, 46]. According to this picture, the characteristic length of loops formed at cosmic time t is given by the scaling relation

$$l \sim \alpha t, \quad (4)$$

with $\alpha \sim 0.1$.

For simplicity and transparency of the formulae obtained in this paper we use several simplifications. We assume cosmology without Λ term with $\Omega_{cdm} + \Omega_b = 1$, the age of the universe $t_0 = (2/3)H_0^{-1} = 3 \times 10^{17}$ s, $t_{eq} \sim 1 \times 10^{12}$ s, and $(1+z)^{3/2} = t_0/t$ for the connection of age t and redshift z in the matter era.

We also assume the fragmentation function for the decay of superheavy X particle into hadrons is

$$dN/dE \propto E^{-2}, \quad (5)$$

while Monte Carlo simulation and the DGLAP method give closer to $E^{-1.92}$ [49].

These simplifications give us a great advantage in understanding the dependence of calculated physical quantities on the basic parameters of our model, in particular on fundamental string parameter η . Our aim in this paper is to obtain the order of magnitude of the flux of UHE neutrinos and to indicate the signatures of the model. We believe our simplified model assumptions are justified, given the uncertainties of string evolution and of the evolution of cosmic magnetic fields.

II. PARTICLE EMISSION FROM SUPERCONDUCTING STRINGS

A. Particle bursts from cusps

As first shown by Witten [35], cosmic strings are superconducting in many elementary-particle models. As they oscillate in cosmic magnetic fields, such strings develop electric currents. Assuming that the string loop size is smaller than the coherence length of the field $l \lesssim l_B \sim 1Mpc$, the electric current can be estimated as [22, 35]

$$J \sim 0.1e^2Bl. \quad (6)$$

Particles are ejected from highly accelerated parts of superconducting strings, called cusps, where large electric currents can be induced [50, 51]. The current near a cusp region is boosted as

$$J_{cusp} \sim \gamma_c J, \quad (7)$$

where J is the current away from the cusp region and γ_c is the Lorentz factor of the corresponding string segment. Particles are ejected from portions of the string that develop Lorentz factors

$$\gamma_c \sim J_{max}/J, \quad (8)$$

where the current reaches the critical value J_{max} . This maximum current is model-dependent, but is bounded by $J_{max} \lesssim e\eta$, where η is the symmetry breaking scale of the string and $e \sim 0.1$ is the elementary electric charge in Gaussian units, renormalized to take into account self-inductance [22].

One may parametrize J_{max} by introducing the parameter $i_c < 1$:

$$J_{max} = i_c e\eta, \quad (9)$$

If the charge carrier is a superheavy particle X with mass m_X , the case which will be considered here, one may use ϵ_X^r for the energy of X -particle in the rest system of the cusp and ϵ_X in the laboratory system. Then $\epsilon_X^r = \gamma m_X = i_c \eta$ and

$$\epsilon_X \sim i_c \gamma_c \eta, \quad (10)$$

respectively, where γ is the average Lorentz factor of X-particle in the rest system of the cusp. In Eq. (10) we took into account that the energy of X-particle in the laboratory system is boosted by the Lorentz factor of the cusp γ_c .

The number of X particles per unit invariant length of the string is $\sim J/e$, and the segment that develops Lorentz factor γ_c includes a fraction $1/\gamma_c$ of the total invariant length l of the loop. Hence, the number of X particles ejected in one cusp event (burst) is

$$N_X^b \sim (J/e)(l/\gamma_c) \sim J^2 l / e J_{max}. \quad (11)$$

The oscillation period of the loop is $l/2$, so assuming one cusp per oscillation, the average number of X particles emitted per unit time is

$$\dot{N}_X \sim 2J^2 / e J_{max}, \quad (12)$$

and the luminosity of the loop is

$$L_{tot} \sim \dot{N}_X \epsilon_X. \quad (13)$$

The X particles are short-lived. They decay producing the parton cascade which is developed due to parton splitting in the perturbative regime, until at the confinement radius the partons are converted into hadrons, mostly pions and kaons, which then decay producing gamma rays, neutrinos, and electrons. These particles together with less numerous nucleons give the observational signatures of superconducting cusps.

The neutrino spectrum at present epoch $z = 0$, produced by the decay of one X-particle with energy $\epsilon_X \sim i_c \gamma_c \eta$ at epoch z can be calculated using the fragmentation function (5) for an X-particle at rest:

$$\xi_\nu(E) \approx \frac{i_c \eta \gamma_c}{2(1+z) \ln(E_{max}^{rest}/E_{min}^{rest})} \frac{1}{E^2}, \quad (14)$$

where E_{max}^{rest} and E_{min}^{rest} are the maximum and minimum neutrino energies in the rest system of X-particle.

Particle emission from a cusp occurs within a narrow cone of opening angle

$$\theta_c \sim \gamma_c^{-1} \sim J/J_{max} \quad (15)$$

The duration of a cusp event is [51]

$$t_{burst} \sim l \gamma_c^{-3} \quad (16)$$

B. Superconducting loops in the universe

In any horizon-size volume of the universe at arbitrary time there are a few long strings crossing the volume and a large number of small closed loops. As loops oscillate under the force of string tension, they lose energy by emitting gravitational waves at the rate

$$\dot{E}_g \sim \Gamma G \mu^2, \quad (17)$$

where $\mu \sim \eta^2$ is the string mass per unit length, $G = 1/m_{Pl}^2$ is the gravitational constant and $\Gamma \sim 50$ is a numerical coefficient.

The number density of loops with lengths in the interval from l to $l + dl$ at time t can be expressed as $n(l, t)dl$. Of greatest interest to us are the loops that formed during the radiation era $t < t_{eq}$ and still survive at $t > t_{eq}$. The density of such loops at time t is given by [22]

$$n(l, t)dl \sim t_{eq}^{1/2} t^{-2} l^{-5/2} dl, \quad (18)$$

in the range from the minimum length l_{min} to the maximum length $l \sim \alpha t_{eq}$, where

$$l_{min} \sim \Gamma G \mu t \sim 3 \times 10^{11} \eta_{10}^2 (1+z)^{-3/2} \text{cm} \quad (19)$$

and $\eta_{10} = \eta/10^{10}$ GeV. Here and below we assume that the loop length parameter in (4) is $\alpha \sim 0.1$, as suggested by simulations [45, 46]. Loops of the minimum length are of most importance in our calculations because they are the most numerous.

For a loop of length l at redshift z , the Lorentz factor at the cusp γ_c can be expressed as

$$\gamma_c = \frac{J_{cusp}}{J} = \frac{i_c e \eta}{0.1 e^2 B l} = \gamma_c(l_{min}) \frac{l_{min}}{l} \quad (20)$$

where $\gamma_c(l_{min}) = \gamma_0(1+z)^{3/2}$ and

$$\gamma_0 = \frac{10 i_c \eta}{e B t_0 \Gamma G \mu} = \frac{1.1 \times 10^{12} i_c}{B_{-6} \eta_{10}} \quad (21)$$

where B_{-6} is the magnetic field in microgauss.

C. Limits on η

The string motion is overdamped at early cosmic times, as a result of friction due to particle scattering on moving strings. The friction-dominated epoch ends at

$$t_* \sim (G\mu)^{-2} t_p, \quad (22)$$

where t_p is the Planck time. In the above analysis we have assumed that loops of interest to us are formed at $t > t_*$. The corresponding condition,

$$\Gamma G \mu t_0 / \alpha \gtrsim t_*, \quad (23)$$

yields

$$\eta \gtrsim 10^9 \text{ GeV}. \quad (24)$$

For strings with $\eta < 10^9$ GeV, loops of the size given by (19) never form. Instead, the smallest loops are those that form at time t_* with length

$$l_{min} \sim \alpha t_*, \quad (25)$$

and then survive until the present day.

We should also verify that energy losses due to particle emission and to electromagnetic radiation in recent epochs (after magnetic fields have been generated) are sufficiently small, so the lifetimes of the loops (which we estimated assuming that gravitational radiation is the dominant energy loss mechanism) are not significantly modified.

The average rate of energy loss due to particle emission is

$$\dot{E}_{part} \sim f_B \dot{N}_X \epsilon_X \sim 2f_B J J_{max} / e^2 \quad (26)$$

where we have used Eqs. (12) and (10). The electromagnetic radiation power is smaller by a factor $e^2 \sim 10^{-2}$.

The factor f_B in Eq. (26) is the filling factor – the fraction of space filled with the magnetic field. It gives the fraction of time that cosmic string loops spend in magnetized regions. We assume that loop velocities are sufficiently high that they do not get captured in magnetized cosmic structures (such as galaxy clusters or LSS filaments). To justify this assumption, we note that particle emission can start only after the cosmic magnetic fields are generated, that is, at $z \sim 3$ or so. Before that, gravitational radiation is the dominant energy loss mechanism, and the loops are accelerated to high speeds by the gravitational rocket effect [52, 53]. The smallest loops of length (19) have velocities $v \sim 0.1$, certainly large enough to avoid capture.

The particle emission energy rate (26) should be compared to the gravitational radiation rate (17).

The ratio of the two rates is zero at $z > z_{max}$, where $z_{max} \sim 2-3$ is the red-shift of magnetic field production. At $z < z_{max}$ it is given by

$$\dot{E}_{part} / \dot{E}_g \sim 50 f_{-3} B_{-6} i_c \eta_{10}^{-1} \left(\frac{l}{l_{min}} \right) (1+z)^{-3/2}. \quad (27)$$

where $f_{-3} = f_B / 10^{-3}$ and l_{min} is given by (19).

If particle emission is the dominant energy loss mechanism, then the lifetime of a loop is

$$\tau_{part} \sim \frac{\mu l}{\dot{E}_{part}} \sim \frac{5\eta}{e i_c f_B B} \sim 0.025 \frac{t_0 \eta_{10}}{f_{-3} B_{-6} i_c}. \quad (28)$$

Note that τ is independent of l . This means that all loops surviving from the radiation era decay at about the same time.

For the time being, we shall assume that particle radiation is subdominant. We shall discuss the opposite regime in Section II.G.

D. Rate of cusp events

The rate of observable cusp bursts (i.e., the bursts whose spot hits the Earth) is given by

$$d\dot{N}_b = f_B \frac{d\Omega}{4\pi} \nu(l, z) dl \frac{dV(z)}{1+z} \quad (29)$$

where, as before, f_B is the fraction of space with magnetic field B , $d\Omega = 2\pi\theta d\theta$ is the solid angle element, with θ limited by the angle of cusp emission $\theta_c \sim 1/\gamma_c$; $\nu(l, z) = n(l, z)/(l/2)$ is the frequency of the bursts with $n(l, z)$ given by Eq. (18), and $dV(z)$ is a proper volume of space limited by redshifts z and $z + dz$,

$$dV(z) = 54\pi t_0^3 [(1+z)^{1/2} - 1]^2 (1+z)^{-11/2} dz. \quad (30)$$

Integrating Eq. (29) over θ , l and z , we obtain

$$\dot{N}_b = 54\pi(t_{eq}t_0)^{1/2}(\Gamma G\mu)^{-1/2}(e/10i_c\eta)^2 \int_0^{z_{max}} dz \frac{[(1+z)^{1/2} - 1]^2}{(1+z)^{11/4}} f_B(z) B^2(z), \quad (31)$$

where z_{max} is the redshift at which the magnetic fields are generated. Since the earth is opaque to neutrinos with the energies we are considering, only half of these bursts can actually be detected by any given detector at the surface of the earth or using the atmosphere.

The value of the integral in (31) depends on one's assumptions about the evolution of the magnetic field B and of the volume fraction f_B . This evolution is not well understood. If we take these values out of the integral in Eq. (31) as the average and characterize them by the effective values of parameters B_{-6} and f_{-3} in the range $0 < z < z_{max}$, then Eq. (31) reduces to

$$\dot{N}_b = 2.7 \times 10^2 \frac{B_{-6}^2 f_{-3}}{i_c^2 \eta_{10}^3} \frac{I}{0.066} \text{ yr}^{-1}, \quad (32)$$

where the integral

$$I = \int_0^{z'} dz \frac{[(1+z)^{1/2} - 1]^2}{(1+z)^{11/4}} = \frac{4}{3}[1 - (1+z')^{-3/4}] - \frac{8}{5}[1 - (1+z')^{-5/4}] + \frac{4}{7}[1 - (1+z')^{-7/4}], \quad (33)$$

is equal to 0.015, 0.042 and 0.066 for $z' = z_{max} = 1, 2$ and 3 , respectively.

The integrand in Eq. (31) includes the product $f_B(z)B^2(z)$. In the calculations of other physical quantities below, similar integrals will have different combinations of $f_B(z)$ and $B(z)$. Nevertheless, we shall assume that the average values taken out of the integral are characterized by approximately the same values of f_{-3} and B_{-6} .

All cosmic structures — galaxies, clusters, and filaments of the large-scale structure — are magnetized and contribute to the rate of cusp bursts. In the recent epoch, $z \lesssim 1$, the dominant contribution is given by clusters of galaxies with $B_{-6}^2 f_{-3} \sim 1$. The magnetic fields of galaxies have about the same magnitude, but the corresponding filling factor f_B is orders of magnitude smaller. We shall assume that this holds in the entire interval $0 < z < z_{max}$. The sources in our model are then essentially clusters of galaxies.

E. Diffuse flux of UHE neutrinos

The diffuse differential neutrino flux, summed over all produced neutrino flavors, is given by the formula

$$J_\nu(E) = \frac{1}{4\pi} \int d\dot{N}_b N_X^b \xi_\nu(E) \frac{1}{\Omega_{jet} r^2(z)}, \quad (34)$$

where $d\dot{N}_b$ is the rate of cusp bursts (29), N_X^b is the number of X particles produced per burst, given by Eq. (11), $\xi_\nu(E)$ is the neutrino spectrum produced by the decay of one X -particle, given by (14),

$$\Omega_{jet} = \pi\theta_c^2 = \frac{\pi}{\gamma_c^2}, \quad (35)$$

$$r(z) = 3t_0[1 - (1+z)^{-1/2}] \quad (36)$$

is the distance between a source at redshift z and the observation point at $z = 0$, and $\Omega_{jet} r^2$ is the area of the burst spot at the Earth from a source at redshift z .

Using expressions (18) and (30), and assuming that the product $f_B(z)B(z)$ does not change much in the interval $0 < z < z_{max}$, we obtain²

$$E^2 J_\nu(E) = \frac{0.3 i_c m_{pl} (t_{eq}/t_0)^{1/2} (eBt_0^2) f_B}{7\pi(\Gamma)^{1/2} t_0 (ct_0)^2 \ln(E_{max}^{rest}/E_{min}^{rest})} [1 - (1 + z_{max})^{-7/4}]. \quad (37)$$

Numerically, this gives for the neutrino flux summed over neutrino flavors

$$E^2 J_\nu(E) = 6.6 \times 10^{-8} i_c B_{-6} f_{-3} \text{ GeV cm}^{-2} \text{ s}^{-1} \text{ sr}^{-1}, \quad (38)$$

where we have set $z_{max} = 3$ and estimated the logarithmic factor as ~ 30 .

For $i_c \sim 1$, the flux (38) is close to the cascade upper limit shown in Figure 1. Notice that the diffuse neutrino flux (37) does not depend on η . The neutrino flux must correlate with clusters of galaxies.

To detect this flux, we need to monitor a target with some large mass M . The effective cross-section of the detector is then

$$\Sigma = \sigma_{\nu N} M / m_N \quad (39)$$

where $\sigma_{\nu N} \sim 3 \times 10^{-32} \text{ cm}^2$ is the neutrino-nucleon cross section at $E \gtrsim 10^{10} \text{ GeV}$ and m_N the mass of a nucleon. Because of the opacity of the earth, the detector will see solid angle about $2\pi \text{ sr}$. The detection rate of particles with energy above E is

$$2\pi E J_\nu(E) \Sigma \approx 23 \left(\frac{M}{10^{18} g} \right) \left(\frac{10^{10} \text{ GeV}}{E} \right) i_c B_{-6} f_{-3} \text{ yr}^{-1} \quad (40)$$

In the case of JEM-EUSO in tilt mode, $M \sim 5 \times 10^{18} g$, and thus we expect about $100 i_c$ detections per year, so events can be expected for $i_c \gtrsim 0.01$.

F. Neutrino fluence and the number of neutrinos detected from a burst

The fluence of neutrinos incident on the detector from a burst at redshift z can be calculated as

$$\Phi(> E) = \frac{N_X^b \xi_\nu(> E)}{\Omega_{jet} r^2(z)} \quad (41)$$

Consider a neutrino burst from a loop of length l at redshift z . Using N_X^b from (11), l_{min} from (19) and $\xi_\nu(> E)$ from (14), we obtain for a loop of any length l ,

$$\Phi(> E) \approx \frac{10 i_c^3 \eta^3}{18\pi e B t_0^2 E \ln(E_{max}^{rest}/E_{min}^{rest}) [(1+z)^{1/2} - 1]^2}, \quad (42)$$

which numerically results in

$$\Phi(> E) \approx 1.2 \times 10^{-2} \frac{i_c^3 \eta_{10}^3}{B_{-6}} \left(\frac{10^{10} \text{ GeV}}{E} \right) \frac{1}{[(1+z)^{1/2} - 1]^2} \text{ km}^{-2} \quad (43)$$

² We note that numerical simulations of the magnetic field evolution performed by Ryu et al. [54] do indicate that the space average of the magnetic field $\langle B(z) \rangle = f_B(z)B(z)$ remains roughly constant at $\sim 10^{-9} \text{ G}$ for $0 < z \lesssim 3$ and decreases at larger values of z . The effective values B_{-6} and f_{-3} could be different from those in Eq. (32) for the rate of bursts, but we neglect the possible difference.

The number of neutrinos detected in a burst is

$$N_\nu^{det} \sim \Phi(> E)\Sigma \quad (44)$$

With $M \sim 5 \times 10^{18}g$ as above,

$$N_\nu^{det}(> E) \approx 0.11 \frac{10^{10} \text{ GeV}}{E} \frac{i_c^3 \eta_{10}^3}{B_{-6}} \frac{1}{[(1+z)^{1/2} - 1]^2} \quad (45)$$

Therefore, for a certain range of $i_c \eta_{10}$ values and source redshifts z , multiple neutrinos can be detected as parallel tracks from a single burst. For example, for $i_c \eta_{10} \sim 3$, and $z \sim 1$, $N_\nu^{det} \sim 17$.

For neutrino energies of interest, $E_\nu \gtrsim 1 \times 10^{20}$ eV, the neutrino Lorentz factor is so large that there is practically no arrival delay for neutrinos with smaller energies. All neutrinos from a burst arrive simultaneously and produce atmospheric showers with parallel axes, separated by large distances.

For other sets of parameters $N_\nu^{det} < 1$, i.e. only one neutrino from a burst (or no neutrino) is detectable. As η increases, the rate of bursts (32) diminishes while the number of neutrinos per burst increases, so that the total neutrino flux remains unchanged. The rate of detected neutrino bursts with the number of detected neutrinos $N_\nu^{det} > \zeta$ for each burst, is given by Eqs (32) and (33), with z_{max} determined by $N_\nu^{det}(> E, z_{max}) = \zeta$. Using Eq. (45) we obtain for $x_{max} \equiv (1 + z_{max})$:

$$x_{max}(> E, \zeta) = \left[1 + \left(\frac{0.11 i_c^3 \eta_{10}^3 10^{10} \text{ GeV}}{\zeta B_{-6} E} \right)^{1/2} \right]^2, \quad (46)$$

if (46) is less than 4, and $x_{max} = 4$ if (46) is larger than 4. Introducing in Eq. (32) coefficient 1/2 which approximately takes into account the absorption of UHE neutrinos crossing the Earth we obtain for the rate of detected bursts with $N_\nu^{det} \geq \zeta$

$$\dot{N}_b^{det}(\geq \zeta) = 2.1 \times 10^3 \frac{f_{-3} B_{-6}^2}{i_c^2 \eta_{10}^3} I(z_{max}) \text{ yr}^{-1}, \quad (47)$$

where $I(z_{max})$ is given by Eq. (33) with z_{max} from Eq. (46).

In Fig. 2, we have shaded the region of the parameter space (η, i_c) corresponding to a detectable flux of neutrinos. Curved lines in the figure mark the regions where we expect a burst with a given multiplicity of neutrinos, $\zeta = 2, 3$ or 10, detected simultaneously by a detector with the parameters of JEM-EUSO tilted. To the left of the 2-neutrino-burst line, only a diffuse flux of single neutrinos can be observed. This flux depends only on i_c , and the vertical left boundary of the shaded region marks the value of i_c at which it drops below one particle detected per year.

Note that the regions shown for multiple events are those where we expect at least one burst per year whose average multiplicity is the given ζ or more. But it is possible even if the parameters are to the left of the $\zeta = 2$ line that we would happen to observe multiple neutrinos from a single burst, which would give a clear signature of neutrino-jet emission from cusps.

Another quantity of interest is the *rate of detected neutrinos* $f_\nu(\geq \zeta)$ in the events with neutrino multiplicity greater than ζ . It is given by

$$f_\nu(\geq \zeta) = \frac{1}{2} \int \frac{f_B}{2} \frac{1}{\gamma_c^2} \frac{n(l, z) dl}{l} \frac{dV(z)}{1+z} N_\nu^{det}(> E, z, l). \quad (48)$$

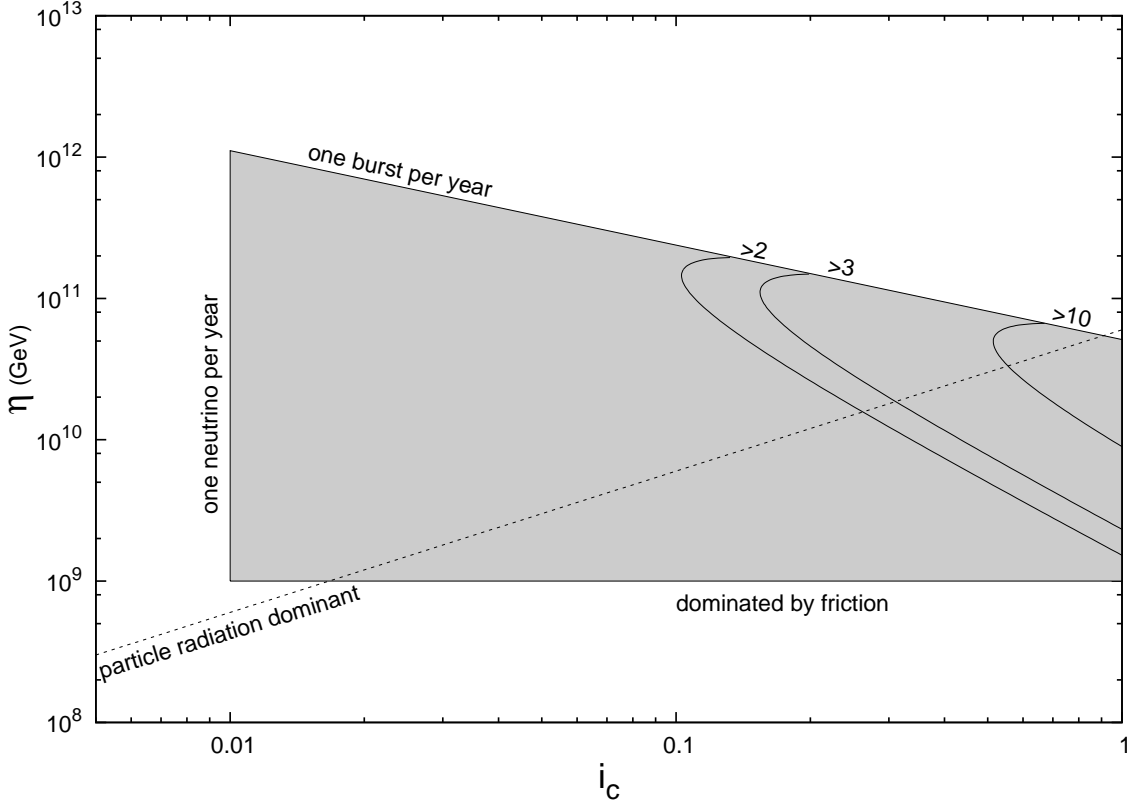


FIG. 2: The region of parameter space where neutrinos can be seen by a detector with the parameters of JEM-EUSO. The curved lines show the left edges of the regions in which bursts containing at least 2, 3, and 10 neutrinos can be expected at least once per year. Below the dotted line, particle radiation is the dominant channel of energy loss from loops.

The important feature of the calculations is the independence of $N_\nu^{det}(> E, z, l)$ from l . This allows us to integrate over l in Eq. (48) to obtain

$$f_\nu(\geq \zeta) = 2.1 \times 10^3 \frac{f_{-3} B_{-6}^2}{i_c^2 \eta_{10}^3} \int_0^{z_{max}(\zeta)} dz (1+z)^{-\frac{11}{4}} [(1+z)^{1/2} - 1]^2 N_\nu^{det}(> E, z), \quad (49)$$

where $z_{max}(\zeta)$ is given by Eq. (46). Using Eq. (45) for $N_\nu^{det}(> E, z)$ results in

$$f_\nu(\geq \zeta) = 1.3 \times 10^2 i_c f_{-3} B_{-6} [1 - x_{max}^{-7/4}(i_c, \eta_{10})] \text{ yr}^{-1}. \quad (50)$$

for $E > 1 \times 10^{19}$ eV. The asymptotic expression at $0.11 i_c^3 \eta_{10}^3 / B_{-6} \zeta \ll 1$ gives

$$f_\nu(\geq \zeta) = \frac{1.5 \times 10^2}{\sqrt{\zeta}} i_c^{5/2} \eta_{10}^{3/2} B_{-6}^{1/2} \text{ yr}^{-1}. \quad (51)$$

G. Neutrino fluxes in the particle-emission dominated regime

So far we have assumed that gravitational radiation is the dominant energy loss mechanism of strings. In the opposite regime, where the particle emission energy losses dominate,

the loop's lifetime τ_{part} is independent of its length and is given by Eq. (28). We shall analyze this regime in the present section.

As before, we shall adopt the idealized model where the magnetic field B is turned on at time $t = t_B$, corresponding to redshift z_{max} ,

$$t_B \sim t_0(1 + z_{max})^{-3/2}. \quad (52)$$

The loops decay at the time $t_{dec} \sim t_B + \tau_{part}$. The rate of observable bursts \dot{N}_b is given by Eq. (32) with I from Eq. (33), where the integration is taken between z_{dec} and z_{max} and z_{dec} is the redshift corresponding to the time t_{dec} .

If $\tau_{part} \gtrsim t_B$, the redshift z_{dec} is significantly different from z_{max} , with $\Delta z = z_{max} - z_{dec} \gtrsim 1$, and the value of I is not much different from that evaluated in Sec. II.D. This is an intermediate regime, in which the results we obtained in Sections II.D and II.E for the rate of bursts and for the diffuse flux can still be used as order of magnitude estimates.

For $\tau_{part} \ll t_B$, the loops lose all their energy to particle emission in less than a Hubble time. The condition $\tau_{part} \sim t_B$ can also be expressed as $\dot{E}_{part}/\dot{E}_g(z_{max}) \sim 1$. Using Eq. (27) with $z_{max} \sim 3$, we find this condition is met for the smallest loops when

$$\eta \sim 6 \times 10^{10} i_c f_{-3} B_{-6} \text{ GeV}. \quad (53)$$

It marks the boundary of the strong particle-emission domination regime and is shown by the inclined dotted line in Fig. 2. Below this line, the results of the preceding sections do not apply even by order of magnitude, but as we shall see, detectable neutrino fluxes can still be produced.

The redshift interval $\Delta z = z_{max} - z_{dec}$ for $\tau_{part} \ll t_B$ can be estimated as

$$\Delta z \approx \frac{2}{3} \frac{\tau_{part}}{t_B} (1 + z_{max}) \ll 1, \quad (54)$$

and the integral I in Eq. (33) is given by

$$I \approx \Delta z \frac{[(1 + z_{max})^{1/2} - 1]^2}{(1 + z_{max})^{11/4}}. \quad (55)$$

With $z_{max} \sim 3$, we have $t_B \sim t_0/8$, and

$$\frac{\tau_{part}}{t_B} \sim 0.2 \frac{\eta_{10}}{f_{-3} B_{-6} i_c}. \quad (56)$$

The rate of bursts that are actually detected, \dot{N}_b^{det} , can be expressed as a product of \dot{N}_b and the probability p_ν^{det} that at least one neutrino from the burst will be detected. This probability is simply related to the average number of detected neutrinos per burst N_ν^{det} , given by Eq. (45),

$$p_\nu^{det} = 1 - \exp(-N_\nu^{det}). \quad (57)$$

For $N_\nu^{det} \ll 1$, we have

$$p_\nu^{det} \approx N_\nu^{det} \quad (58)$$

and again taking $E > 1 \times 10^{19}$ eV,

$$\dot{N}_b^{det} \sim \dot{N}_b N_\nu^{det} \sim \frac{60\eta_{10}}{(1 + z_{max})^{7/4}} yr^{-1} \sim 5\eta_{10} yr^{-1}, \quad (59)$$

where in the last step we have used $z_{max} \sim 3$. Requiring that $\dot{N}_b^{det} \gtrsim 1 \text{ yr}^{-1}$, we obtain the condition

$$\eta \gtrsim 10^9 \text{ GeV}. \quad (60)$$

Note that at the boundary of detectability, where $\eta \sim 10^9 \text{ GeV}$, we always have $N_\nu^{det} \ll 1$, and thus the approximation (58) is justified. This boundary is the lower horizontal line bounding the observable parameter range in Fig. 2. Note also that Eq. (60) coincides with with the condition (24) for the burst-producing loops to be unaffected by friction.

It is interesting to note that the detection rate (59) in the particle-emission dominated regime is independent of i_c and depends only on the symmetry breaking scale η . This is in contrast with Eq. (40) for the case of gravitational radiation dominance, where the rate is proportional to i_c and independent of η .

H. Cascade upper limit on neutrino flux in the superconducting string model

In Subsection I.C of the Introduction, we gave a very general upper limit for UHE neutrino flux. The presence of such a limit does not contradict the existence of stronger upper limits in some particular models with additional assumptions.

In this section, we calculate the energy density of the cascade radiation in our model and compare it with $\omega_{cas} = 2 \times 10^{-6} \text{ eV cm}^{-3}$ allowed by EGRET measurements.

The cascade energy density can be calculated as

$$\omega_{cas} = \int_0^{z_{max}} \frac{dz}{(1+z)^4} \int_{l_{min}(z)}^{l_{max}(z)} dl f_B n(l, t) L_{em}(l, t) \quad (61)$$

where $L_{em}(l, t) \sim \frac{1}{2} L_{tot}(l, t)$ is the loop luminosity in the form of UHE electrons and photons produced by pion decays. The standard calculation (for $z_{max} = 3$) results in

$$\omega_{cas} \approx \frac{1.2 i_c (eB t_0^2) (t_{eq}/t_0)^{1/2} f_B \eta}{7(\Gamma G \mu)^{1/2} t_0^3} [1 - (1 + z_{max})^{-7/4}] \approx 8.3 \times 10^{-7} i_c f_{-3} B_{-6} \text{ eV cm}^{-3} \quad (62)$$

The energy density (62) does not depend on η and since $\omega_{cas} < \omega_{EGRET}$, it respects the general upper limit (3). For $i_c \sim 1$, the predicted neutrino flux (38) is close to the upper limit shown in figure 1.

III. GAMMA-RAY JETS AND SINGLE GAMMA-RAYS FROM THE CUSPS

A. Bursts from loops in the Milky Way

In each galaxy, including the Milky Way, there are approximately N_l loops with $l \gtrsim l_{min}$,

$$N_l \sim n(> l_{min}) V_g \sim 2.5 \times 10^5 \eta_{10}^{-3} V_g / 10^3 \text{ kpc}^3, \quad (63)$$

where V_g is the volume of the magnetized part of the galaxy. A narrow jet of particles emanating from a cusp on such a loop can in principle hit the Earth. The probability of such a catastrophic event is very small because of the smallness of solid angle Ω_{jet} of jet emission. The number of jets hitting an area S on the Earth per unit time does not depend on S if $S \ll \Omega_{jet} r^2$, where r is the distance from the source. This rate is given by

$$\dot{N}_b = PV_g \int dl \frac{2n(l)}{l}, \quad (64)$$

where again we assume one cusp per oscillation, and $P = \Omega_{jet}/4\pi = 1/(4\gamma_c)^2$ is the probability to hit the detector. After the standard calculations, we obtain for $V_g \sim 1 \times 10^3 \text{ kpc}^3$,

$$\dot{N}_b = 1 \times 10^{-13} B_{-6}^2 \eta_{10}^{-3} i_c^{-2} \text{ yr}^{-1}. \quad (65)$$

Thus, for particles propagating rectilinearly, the jets from cusps in our galaxy are unobservable.

The most important components of the galactic jets are photons and neutrinos. A photon jet at the highest energies undergoes widening of the jet angle due to photon absorption in the galactic magnetic field [55]. Absorption of photons, $\gamma + B \rightarrow B + e^+ + e^-$, is followed by energy loss by electrons and positrons in the magnetic field, with the emission of synchrotron photons in directions different from that of the primary photon. This results in the widening of the solid angle Ω_{jet} [55].

The widening of photon jets in the Milky Way is negligible. This can be illustrated by a numerical example. The highest energy of a photon in a jet is $E_\gamma^{max} \sim \gamma_c \eta \sim 10^{31} i_c / B_{-6} \text{ eV}$. Photons with $E_\gamma \geq 10^{25} \text{ eV}$ are absorbed in galactic magnetic fields. The produced electrons and positrons with $E_e \sim 10^{25} \text{ eV}$ have lifetime $\tau \sim 10^3 \text{ s}$ for synchrotron energy losses and attenuation length $l_{att} \sim 3 \times 10^{13} \text{ cm}$. Since the Larmor radius of such electrons is $r_L \sim 3 \times 10^{28} \text{ cm}$, the deflection angle $\theta \sim l_{att}/r_L \sim 10^{-15}$ is of no consequence.

B. Cascade gamma-radiation from Virgo cluster

As was discussed above, the photon jets from the galactic cusps are not widening and thus are invisible. For cusps at large distances, the widening of the photon jet efficiently occurs in the cascading on CMB photons, $\gamma + \gamma_{CMB} \rightarrow e^+ + e^-$, $e + \gamma_{CMB} \rightarrow e' + \gamma'$ etc., and the source can be seen in gamma-radiation. As in the case of diffuse cascade radiation (see section I.C), all primary photons with energy higher than the absorption energy ϵ_a are absorbed on CMB radiation and converted into low-energy cascade photons. Thus, cusps can be seen in $100 \text{ GeV} - 100 \text{ TeV}$ gamma radiation, similar to the sources of UHE protons which can be seen in TeV gamma-radiation [56].

The nearest source from which this radiation can be expected is the Virgo cluster. It is located at distance $r = 18 \text{ Mpc}$, and the number of loops within the core of radius $R_c \sim 3 \text{ Mpc}$, where a magnetic field $B \sim 10^{-6} \text{ G}$ can be reliably assumed, can reach $n_l R_c^3 \sim 7 \times 10^{12} \eta_{10}^{-3}$, with the luminosity in $\gamma e^+ e^-$ component for each loop $L_{loop}^\gamma \sim 2 \times 10^{29} i_c \eta_{10}^3 B_{-6} \text{ erg s}^{-1}$. Half of this energy goes into cascade radiation, $L_{cas} \sim 0.5 L_{loop}^\gamma$.

The spectrum of the cascade photons at distance $r \sim 20 \text{ Mpc}$ has two characteristic energies [40]: the absorption energy $\epsilon_a \sim 100 \text{ TeV}$ and the energy ϵ_x . The latter is the energy of a photon produced by an electron born in $\gamma + \gamma_{CMB} \rightarrow e^+ + e^-$ scattering by a photon with $E_\gamma = \epsilon_a$. The energy of this electron is $E_e \sim 0.5\epsilon_a \sim 50 \text{ TeV}$ and the second characteristic energy is $\epsilon_x \sim 20 \text{ TeV}$ for $r \sim 20 \text{ Mpc}$.

The spectrum of cascade photons at observation is calculated in [40] as

$$J_\gamma(E_\gamma) = \begin{cases} K(E_\gamma/\epsilon_x)^{-3/2}, & E_\gamma \leq \epsilon_x \\ K(E_\gamma/\epsilon_x)^{-2.0}, & \epsilon_x \leq E_\gamma \leq \epsilon_a \end{cases} \quad (66)$$

The spectrum constant K in (66) can be expressed in terms of the cascade luminosity L_{cas} and the distance to the source r as

$$K = \frac{L_{cas}}{\Omega_{eff} r^2} \frac{1}{\epsilon_x^2 (2 + \ln(\epsilon_a/\epsilon_x))}, \quad (67)$$

where Ω_{eff} is the effective solid angle produced by scattering of cascade electron in extragalactic magnetic field. In case of full isotropization $\Omega_{eff} \sim 4\pi$. Cascade luminosity can be estimated as 1/4 of the total luminosity of cusps in a cluster, $L_{cas} \sim \frac{1}{4} L_{loop} N_{loop}$. Using $L_{loop} = 4.4 \times 10^{29} i_c \eta_{10}^3 B_{-6} \text{ erg s}^{-1}$ and $N_{loop} \sim 2.5 \times 10^{11} \eta_{10}^{-3}$, valid for a cluster core with $R_c \sim 3 \text{ Mpc}$, one obtains for the flux

$$J_\gamma(> \epsilon_x) = \int_{\epsilon_x}^{\epsilon_a} dE_\gamma J_\gamma(E_\gamma) \sim 1 \times 10^{-13} i_c B_{-6} (R_c/3 \text{ Mpc})^3 \text{ cm}^{-2} \text{ s}^{-1} \quad (68)$$

which is marginally detectable by present telescopes. Note that L_{cas} and the flux J_γ do not depend on η . We consider the estimate (68) as a very rough indication of detectability of the gamma-ray flux from the Virgo cluster. Much more accurate calculations are needed for a reliable prediction of this flux.

IV. UHE PROTONS FROM SUPERCONDUCTING STRINGS

The cusps of superconducting strings in clusters of galaxies produce UHE nucleons at fragmentation of parton jets with a fraction of nucleons $\epsilon_N = 0.12$ [33] relative to the total number of hadrons. The generation rate $Q_p(\Gamma_p)$ of UHE protons with Lorentz factor Γ_p per unit comoving volume and unit time can be expressed through emissivity,

$$\mathcal{L}_0 = \int_{\Gamma_p^{min}}^{\Gamma_p^{max}} d\Gamma_p m_N \Gamma_p Q_p(\Gamma_p), \quad (69)$$

where the emissivity \mathcal{L}_0 is the energy released in UHE protons at $z = 0$ per unit comoving volume per unit time, Γ_p^{max} and $\Gamma_p^{min} \sim 1$ are the maximum and minimum Lorentz factors of the protons, respectively, and m_N is the nucleon mass. For a power-law generation spectrum $Q_p(\Gamma_p) \sim \Gamma_p^{-2}$, we have

$$Q_p(\Gamma_p) = \frac{\mathcal{L}_0}{m_N \ln \Gamma_p^{max}} \Gamma_p^{-2}. \quad (70)$$

The emissivity is calculated as

$$\mathcal{L}_0 = \epsilon_N f_B \int_{l_{min}}^{l_{max}} dl n(l) L_{tot}^{cusp}(l), \quad (71)$$

where l_{min} is given by (19), while $n(l)$ and L_{cusp} are given by (18) and (13) respectively. For L_{tot}^{cusp} one readily obtains

$$L_{tot}^{cusp} = \frac{J^2 l i_c \gamma_c \eta}{e J_c l/2} = 0.2 i_c e B l \eta, \quad (72)$$

and after a simple calculation we have

$$\mathcal{L}_0 \approx 0.4 i_c \epsilon_N f_B \frac{(t_{eq}/t_0)^{1/2} e B t_0^2 \eta}{(\Gamma G \mu)^{1/2}} \frac{1}{t_0 (t_0)^3} \approx 1.4 \times 10^{45} i_c f_{-3} B_{-6} \text{ erg Mpc}^{-3} \text{ yr}^{-1}. \quad (73)$$

One more parameter relevant for the calculation of $Q_p(\Gamma_p)$ is $\Gamma_p^{\max} = E_p^{\max}/m_N$. It can be estimated using $E_p^{\max} \sim 0.1 \epsilon_X$, where $\epsilon_X = i_c \gamma_c \eta$ is the energy of the boosted X particles in the laboratory system, which being estimated for loops of length l_{min} , gives

$$\Gamma_p^{\max} = 1 \times 10^{10} \eta_{10} i_c^2 \frac{1}{\Gamma G \mu} \frac{\eta}{e B t_0} \left(\frac{1 \text{ GeV}}{m_N} \right). \quad (74)$$

Notice that Γ_p^{\max} does not depend on η and that it enters $Q_p(\Gamma_p)$ through $\ln \Gamma_p^{\max}$.

Now we can calculate the space density of UHE protons using the generation rate $Q_p(\Gamma_p)$ given by (70) and taking into account propagation through CMB radiation with the help of the kinetic equation [57, 58]

$$\frac{\partial}{\partial t} n_p(\Gamma_p, t) - \frac{\partial}{\partial \Gamma_p} [b(\Gamma_p, t) n_p(\Gamma_p, t)] = Q_p(\Gamma_p, t), \quad (75)$$

where $b(\Gamma_p, t) = -d\Gamma/dt$ describes energy losses of UHE protons interacting with CMB photons. For $\Gamma \geq 3 \times 10^{10}$, the proton energy losses become large and one can neglect the first term in the lhs of equation (75). Then Eq. (75) becomes stationary and its solution for $t = t_0$ reads

$$n_p(\Gamma_p) = \frac{1}{b(\Gamma_p)} \int_{\Gamma_p}^{\Gamma_p^{\max}} Q_p(\Gamma_p) d\Gamma_p \approx \frac{\mathcal{L}_0}{m_N \Gamma_p b(\Gamma_p) \ln \Gamma_p^{\max}}. \quad (76)$$

In terms of the proton energy $E = m_N \Gamma_p$ and the diffuse flux $J_p(E) = (c/4\pi) n_p(E)$, we have, in the standard form of presentation,

$$E^3 J_p(E) \approx \frac{c}{4\pi} \frac{\mathcal{L}_0}{\ln \Gamma_p^{\max}} \frac{E^2}{b(E)}, \quad (77)$$

where $b(E) = dE/dt$. With $b(E)$ taken from [58] a numerical estimate at $E = 3 \times 10^{19} \text{ eV}$ gives

$$E^3 J_p(E) \approx 1.3 \times 10^{24} i_c f_{-3} B_{-6} \text{ eV}^2 \text{ m}^{-2} \text{ s}^{-1} \text{ sr}^{-1}. \quad (78)$$

With $i_c \sim 1$, the calculated flux (78) coincides well with the measurements at the same energy, e.g., with the HiRes [59] flux $E^3 J_p(E) = 2.0 \times 10^{24} \text{ eV}^2 \text{ m}^{-2} \text{ s}^{-1} \text{ sr}^{-1}$, so the cusp emission may account for the observed events at the highest energies. For $i_c \lesssim 0.1$ the UHE proton flux from superconducting strings is subdominant.

The UHE proton spectrum from superconducting strings has a sharper GZK cutoff than the standard spectrum for homogeneously distributed sources. This is due to the absence of clusters of galaxies in the vicinity of our galaxy. The nearest cluster, Virgo, is located at 18 Mpc from the Milky Way; other clusters are located at much larger distances. Nearby sources affect the spectrum at $E \geq 1 \times 10^{20} \text{ eV}$, where the proton spectrum from superconducting strings is predicted to be steeper than the standard one. The experimental data at present have too low statistics to distinguish the two cases.

In contrast, homogeneously distributed sources such as necklaces [32], give the dominant contribution at $E \geq (7 - 8) \times 10^{19}$ eV in the form of UHE photons, coming from nearby sources. In the case of superconducting strings such component is absent. The UHE photon component from superconducting strings is not dominant at energy lower than 5×10^{19} eV, because absorption of photons at these energies is stronger than for protons.

V. CONCLUSIONS

Superconducting cosmic strings produce high energy particles in the decay of charge carriers, X particles, ejected from the string cusps. The large Lorentz factor γ_c of the cusp boosts the energies of these particles and collimates them in a narrow beam with opening angle $\theta \sim 1/\gamma_c$. The basic string parameter is η , the scale of symmetry breaking, which we parametrize as $\eta = \eta_{10} 10^{10}$ GeV. Another free parameter $i_c \lesssim 1$ determines the critical electric current in the cusp, $J_{max} = i_c e \eta$, and the mean energy of the charge carriers X escaping from the string, $\epsilon_X = i_c \gamma_c \eta$.

The astrophysical parameter which determines the electric current induced in the string is the magnitude of the magnetic field B in the relevant cosmic structures. The fraction f_B of the universe occupied by magnetic field B determines the flux of high-energy particles produced by superconducting strings. The most favorable values of B and f_B for the generation of a large flux of UHE neutrinos are $B \sim 10^{-6}$ G and $f_B \sim 10^{-3}$. They correspond to clusters of galaxies.

The main uncertainties of our model are related to the uncertainties in our understanding of the evolution of cosmic strings and of the origin and evolution of cosmic magnetic fields. On the cosmic string side, the key unknown quantity is the parameter α which sets the characteristic length of string loops in Eq. (4). Here, we used the value of $\alpha \sim 0.1$, as suggested by numerical simulations in Refs. [45, 46]. We have also disregarded the effects of loop fragmentation. Toward the end of its life, the loop's configuration may be sufficiently modified by radiation back-reaction that the loop will self-intersect and break up into smaller pieces. These smaller loops will have more frequent cusps, shorter lifetimes, higher velocities, and smaller induced currents. The effect of such loops on the neutrino fluxes is hard to assess without a quantitative model of loop fragmentation. This will have to await the next generation of string evolution simulations.

On the astrophysical side, basically unknown is the cosmological evolution of the magnetic field parameters $f_B(z)$ and $B(z)$ in the redshift interval $0 < z < z_{max}$, where $z_{max} \sim 2 - 3$ is the redshift when the magnetic field was generated. For the space average value $\langle f_B(z) B(z) \rangle$ we use the numerical simulation by Ryu et al. [54], according to which this value remains roughly constant at $0 < z < 3$. Some important quantities, such as the diffuse neutrino flux $J_\nu(E)$, the cascade energy density ω_{cas} , and the UHE proton emissivity are determined by the evolution of the product $f_B(z) B(z)$. However, some other quantities, such as the rate of neutrino bursts and fluence depend on the evolution of $f_B(z)$ and $B(z)$ in other combinations. In these cases we consider the parameters f_{-3} and B_{-6} as effective values, using $f_{-3} \sim B_{-6} \sim 1$.

In addition, we adopted the following simplifying assumptions. The Lorentz factor of the cusp is characterized by a single fixed value γ_c , while in reality there is a distribution of Lorentz factors along the cusp. The spectrum of particles in a jet is approximated as E^{-2} , while a QCD calculation [49] gives a spectrum which is not a power law, with the best power-law fit as $E^{-1.92}$. We use cosmology with $\Lambda = 0$. The spectrum of photons from Virgo cluster

and the diffuse spectrum of UHE protons are calculated using very rough approximations. Given the uncertainties of string and magnetic field evolution, these simplifications are rather benign. On the other hand, they have the advantage of yielding analytic formulae, which allow us to clearly see the dependence of the results on the parameters involved in the problem. In particular, with the assumed particle spectrum $\sim E^{-2}$, the diffuse flux of neutrinos, the cascade upper limit, the flux of TeV photons from Virgo cluster and the diffuse flux of UHE protons do not depend on η . Since the realistic spectrum is very close to E^{-2} , this means that the quantities listed above depend on η very weakly.

We summarize the results obtained in this work as follows.

As our calculations show, among different sources, such as galaxies, group of galaxies, filaments, etc., the largest diffuse flux is produced by clusters of galaxies with $B \sim 10^{-6} G$ in a cluster core and $f_B \sim 10^{-3}$. The calculated diffuse neutrino flux for three neutrino flavors and for $z_{max} = 3$ is

$$E^2 J_\nu(E) \sim 6.6 \times 10^{-8} i_c f_{-3} B_{-6} \text{ GeV cm}^{-2} \text{ s}^{-1} \text{ sr}^{-1}. \quad (79)$$

This flux respects the cascade upper limit, provided by the energy density of electrons, positrons and photons, which initiate electromagnetic cascades in collisions with CMB photons. The cascade energy density is calculated from Eq. (79) as

$$\omega_{cas} \approx 8.3 \times 10^{-7} i_c f_{-3} B_{-6} \text{ eV cm}^{-3}. \quad (80)$$

and is close to the cascade limit for $i_c \sim 1$. It is the same as given by Eq. (62).

At energies $E \lesssim 10^{22} \text{ eV}$, the flux (79) is detectable by future detectors JEM-EUSO and Auger (South + North). The signature of the superconducting string model is the correlation of neutrinos with clusters of galaxies. We note, however, that the neutrino flux from the nearest cluster, Virgo, is undetectable by the above-mentioned detectors.

Another signature of the model is the possibility of multiple events, when several showers appear simultaneously in the field of view of the detector, e.g. JEM-EUSO. They are produced by neutrinos from the same jet. The time delay in arrival of neutrinos with different energies is negligibly small. Such multiple events are expected to appear for a certain range of parameters, as indicated in Fig. 2.

As an illustration, in Table I we show, for a representative value $\eta = 5 \times 10^{10} \text{ GeV}$, the diffuse neutrino flux, in units of the cascade upper limit J_ν^{max} , the rate of bursts, and the average shower multiplicity for several values of i_c . Note that the bottom row in the table is the *average* multiplicity, that is, the average number of neutrinos detected per burst. For example, the low multiplicity at $i_c = 0.1$ indicates that only a small number (about 5) out of the 220 bursts per year will actually be detected. For $i_c = 1/3$, the average multiplicity is below 1, but Fig. 2 shows that we can expect at least one 2-neutrino burst per year.

A photon jet from the cusp initially propagates together with the neutrino jet, within the same solid angle. However, at large enough distance, photons from the jet can be absorbed in collisions with CMB photon ($\gamma + \gamma_{CMB} \rightarrow e^+ + e^-$), the produced electrons (positrons) emit high-energy photons in inverse-Compton scattering ($e + \gamma_{CMB} \rightarrow e' + \gamma'$), and thus an em cascade develops. Electrons are deflected in magnetic fields, and photon radiation is isotropized. Due to this effect, $10 - 100 \text{ TeV}$ gamma radiation from the nearby cluster of galaxies, Virgo, can be marginally detectable. The corresponding photon flux is given by

$$J_\gamma(> \epsilon_x) \sim 1 \times 10^{-13} i_c B_{-6} \text{ cm}^{-2} \text{ s}^{-1} \quad (81)$$

TABLE I: The diffuse flux $J_\nu(E)$ in units of the cascade upper limit J_ν^{max} for 3 neutrino flavors, found from (3), the rate of neutrino bursts, and the shower multiplicity (the average number of neutrinos detected in one bursts), for $\eta = 5 \times 10^{10}$ GeV, $z_{max} = 3$ and different values of i_c . The multiplicity is shown for neutrinos with $E \gtrsim 10^{10}$ GeV from a burst at $z = 2$.

i_c	1.0	1/2	1/3	0.1
J_ν/J_ν^{max}	0.42	0.21	0.14	0.042
rate of bursts	2.2 yr ⁻¹	8.7 yr ⁻¹	19.6 yr ⁻¹	220 yr ⁻¹
multiplicity	26	3.2	0.95	0.026

where $\epsilon_x \sim 20$ TeV.

In the Milky Way, there may be a large number of loops with radiating cusps, but because of the very small jet opening angle, the probability to observe UHE particle jets coming from these loops is extremely small.

The diffuse flux of UHE protons is suppressed by the small fraction of nucleons produced at decay of X particles (the factor $\epsilon_N = 0.12$ is obtained in MC and DGLAP calculations [49]), and by energy losses of protons interacting with the CMB during propagation. The calculated flux at energy $E \geq 3 \times 10^{19}$ eV is given by the approximate formula

$$E^3 J_p(E) \approx \frac{c}{4\pi} \frac{\mathcal{L}_0}{\ln \Gamma_p^{max}} \frac{E^2}{b(E)} \quad (82)$$

where $b(E) = -dE/dt$ is the energy loss rate of protons, Γ_p^{max} is the maximum Lorentz factor of a proton at production, and \mathcal{L}_0 is the emissivity (energy in the form of protons emitted per unit comoving volume per unit time), given by

$$\mathcal{L}_0 \approx 1.4 \times 10^{45} i_c f_{-3} B_{-6} \text{ erg Mpc}^{-3} \text{ yr}^{-1} \quad (83)$$

For $i_c \sim 1$ and $E \sim 3 \times 10^{19}$ eV, the proton flux can reach the value 1.3×10^{24} eV² m⁻² s⁻¹ sr⁻¹, which can be compared for example with 2×10^{24} eV² m⁻² s⁻¹ sr⁻¹ measured by HiRes [59]. Thus, radiation from cusps may account for observed events at the highest energies. The predicted spectrum at $E > 8 \times 10^{19}$ eV is steeper than the standard UHECR spectrum with homogeneous distribution of sources. The accompanying UHE gamma radiation is very low, due to large distances between the sources (clusters of galaxies).

As already mentioned, practically all predicted quantities, such as the diffuse neutrino flux (79), the cascade energy density (80), the UHE gamma-ray flux from Virgo cluster (81), the diffuse flux of UHE protons (82) and the proton emissivity (83), do not depend on the basic string parameter η . There are only two observable quantities that do, the rate of neutrino bursts \dot{N}_b and the neutrino fluence $\Phi(> E)$:

$$\dot{N}_b \sim 3 \times 10^2 \frac{B_{-6}^2 f_{-3}}{i_c^2 \eta_{10}^3} \text{ yr}^{-1} \quad (84)$$

$$\Phi(> E) \approx 1 \times 10^{-2} \frac{i_c^3 \eta_{10}^3}{B_{-6}} \left(\frac{10^{10} \text{ GeV}}{E} \right) \frac{1}{[(1+z)^{1/2} - 1]^2} \text{ km}^{-2}, \quad (85)$$

As η decreases (at a fixed i_c), the rate of neutrino bursts goes up and the number of neutrinos detected in a burst,

$$N_\nu^{det}(> E) \approx 0.11 \frac{10^{10} \text{ GeV}}{E} \frac{i_c^3 \eta_{10}^3}{B_{-6}} \frac{1}{[(1+z)^{1/2} - 1]^2} \quad (86)$$

goes down, while the product $\dot{N}_b N_\nu^{det}$ remains η -independent.

We have considered here only “regular”, field theory cosmic strings. Recent developments in superstring theory suggest [60–62] that the role of cosmic strings can also be played by fundamental (F) strings and by D -branes. Such strings may be superconducting, in which case they will also emit bursts of relativistic particles from their cusps. The main difference from the case of ordinary strings is that the probability for two intersecting strings to reconnect, which is $p = 1$ for ordinary strings, can be $p < 1$ and even $p \ll 1$ for F or D -strings. A low reconnection probability results in an enhanced density of loops; the particle production by loops is increased correspondingly.

UHE neutrinos from superconducting strings may have three important signatures: correlation with clusters of galaxies, multiple neutrino-induced showers observed simultaneously in the field of view of a detector, e.g. JEM-EUSO, and detection of $\sim 10 \text{ TeV}$ gamma-radiation from Virgo, the nearest cluster of galaxies.

VI. ACKNOWLEDGMENTS

We would like to thank J. J. Blanco-Pillado for useful discussions, and A. Gazizov for preparing Fig. 1 and discussions. This work was supported in part by the National Science Foundation under grants 0353314 and 0457456 (USA), and by the contract ASI-INAF I/088/06/0 for theoretical studies in High Energy Astrophysics (Italy).

-
- [1] See <http://www.jemeuso.riken.jp/>
 - [2] G. Askarian, JETP, **14** (1962) and **21** (1965).
 - [3] D. Saltzberg, Phys. Rev. Lett. **86**, 2802 (2001);
P. W. Gorham et al, Phys. Rev. Lett. **99**, 171101 (2007)
 - [4] P. W. Gorham et al, Phys. Rev. Lett. **93**, 041101 (2004)
 - [5] N. Lehtinen et al, Phys. Rev. D **69**, 013008 (2004)
 - [6] S. W. Barwick et al., Phys. Rev. Lett. **96**, 171101 (2006);
P. W. Gorham et al., arXiv:0812.2715.
 - [7] I. Kravchenko et al, Astrop. Phys., **19**, 15 (2003).
 - [8] V. Berezhinsky and A. Smirnov, Ap. Sp. Sci., **32**, 461 (1975).
 - [9] D. Fargion, Astrophys.J. **570**, 909 (2002), arXiv:astro-ph/0002453.
 - [10] J. Abraham et al (Auger Collaboration), arXiv:0712.1909.
 - [11] V. S. Berezhinsky and G. T. Zatsepin, Phys. Lett **B 28**, 423 (1969); V. S. Berezhinsky and G. T. Zatsepin, Soviet Journal of Nuclear Physics **11**, 111 (1970).
 - [12] K. Greisen, Phys. Rev. Lett. **16**, 748 (1966), G. T. Zatsepin and V. A. Kuzmin, Pisma Zh. Experm. Theor. Phys. **4**, 114 (1966).
 - [13] O. E. Kalashev, V. A. Kuzmin, D. V. Semikoz and G. Sigl, Phys. Rev. D **66**, 063004 (2002).
 - [14] Z. Fodor, S. Katz, A. Ringwald and H. Tu, JCAP **0311**, 015 (2003).

- [15] V. Berezhinsky, A. Gazizov and S. Grigorieva in Proc. of 11th Int. Workshop “Neutrino Telescopes” p. 339-354, ed, by Milla Baldo Ceolin, Venice 2005, astro-ph/0509675.
- [16] D. Hooper, A. Taylor, S. Sarkar, *Astropart.Phys.* **23**, 11 (2005).
- [17] Maximo Ave et al., *Astropart.Phys.* **23**, 19 (2005).
- [18] D. Seckel, T. Stanev, *Phys.Rev.Lett.* **95** 141101 (2005).
- [19] D. Allard et al., *JCAP* 0609, 005 (2006).
- [20] H. Takami, K. Murase, S. Nagataki, K. Sato, arXiv:0704.0979.
- [21] C. T. Hill, D. N. Schramm and T. P. Walker, *Phys. Rev. D* **36**, 1007 (1987).
- [22] A. Vilenkin and E. P. S. Shellard, *Cosmic Strings and Other Topological Defects*, Cambridge University Press, Cambridge, England, 1994.
- [23] P. Bhattacharjee and G. Sigl, *Phys. Rept.* **327**, 109 (2000).
- [24] V. Berezhinsky, P. Blasi, A. Vilenkin, *Phys. Rev. D* **58**, 103515 (1998).
- [25] G. H. MacGibbon and R. H. Brandenberger, *Nucl. Phys. B* **331**, 153 (1990).
- [26] J. J. Blanco-Pillado and K. D. Olum, *Phys. Rev. D* **59**, 063508 (1999).
- [27] K. D. Olum and J. J. Blanco-Pillado, *Phys. Rev. D* **60**, 023503 (1999).
- [28] P. Bhattacharjee and G. Sigl, *Phys. Rev. D* **51**, 4079 (1995).
- [29] C. T. Hill, *Nucl. Phys. B* **224**, 469 (1983).
- [30] J. J. Blanco-Pillado and K. D. Olum, *Phys. Rev. D* **60**, 083001 (1999).
- [31] D. V. Semikoz for the Auger Collaboration, arXiv:0706.2690.
- [32] V. Berezhinsky, A. Vilenkin, *Phys. Rev. Lett.* **79**, 5202 (1997).
- [33] R. Aloisio, V. Berezhinsky, M. Kachelriess, *Phys. Rev. D*, **69**, 094023 (2004)
- [34] J. J. Blanco-Pillado and K. Olum, arXiv:0707.3460
- [35] E. Witten, *Nucl. Phys. B* **249**, 557 (1985).
- [36] V. Berezhinsky, M. Kachelriess, A. Vilenkin, *Phys. Rev. Lett.* **79**, 4302 (1997).
- [37] V. A. Kuzmin, V. A. Rubakov, *Phys. Atom. Nukl.* **61** 1028 (1998) [*Yad. Phys.* **61**, 1122 (1998)].
- [38] E. W. Kolb, D. J. H. Chung, A. Riotto, *Phys. Rev. Lett.* **81**, 4048 (1998).
- [39] V. A. Kuzmin, I. I. Tkachev, *JETP Lett.* **68** (1998) 271-275.
- [40] V. S. Berezhinsky, S. V. Bulanov, V. A. Dogiel, V. L. Ginzburg and V. S. Ptuskin, *Astrophysics of Cosmic Rays*, North-Holland 1990.
- [41] P. Sreekumar et al. [EGRET collaboration], *Astroph. J.* **494**, 523 (1998).
- [42] V. Berezhinsky, *Nucl. Phys. B (Proc. Suppl.)* **151**, 260 (2006).
- [43] C. J. A. Martins and E. P. S. Shellard, *Phys. Rev. D* **73**, 043515 (2006)
- [44] C. Ringeval, M. Sakellariadou and F. Bouchet, *JCAP* **0702**, 023 (2007)
- [45] V. Vanchurin, K. D. Olum and A. Vilenkin, *Phys. Rev. D* **74**, 063527 (2006)
- [46] K. D. Olum and V. Vanchurin, *Phys. Rev. D* **75**, 063521 (2007)
- [47] F. Dubath, J. Polchinski and J. V. Rocha, *Phys. Rev. D* **77**, 123528 (2008)
- [48] V. Vanchurin, *Phys. Rev. D* **77**, 063532 (2008)
- [49] V. Berezhinsky, M. Kachelriess, *Phys. Rev. D* **63**, 034007 (2001).
R. Aloisio, V. Berezhinsky and M. Kachelriess, *Phys. Rev. D* **69**, 094023 (2004).
S. Sarkar, R. Toldra, *Nucl. Phys. B* **621**, 495 (2002).
C. Barbot, M. Drees, *Phys. Lett. B* **533**, 107 (2002).
- [50] D.N. Spergel, W.H. Press and J. Goodman, *Nucl. Phys.* **B291**, 847 (1987).
- [51] A. Babul, B. Paczynski and D. Spergel, *Ap. J. Lett.* **316**, L49 (1987).
- [52] T. Vachaspati and A. Vilenkin, *Phys. Rev.* **D31**, 3052 (1985).
- [53] C.J. Hogan and M.J. Rees, *Nature* **311**, 109 (1984).

- [54] D. Ryu, H. Kang, J. Cho and S. Das, *Science* **320**, 909 (2008).
- [55] V. S. Berezinsky, *Sov. Phys. Nucl. Phys.* **11**, 399 (1970).
- [56] C. Ferrigno, P. Blasi, D. De Marco, *Astrop. Phys.* **23**, 211 (2005).
- [57] M.S. Longaire, *High Energy Astrophysics*, Cambridge University Press, 1987.
- [58] V. Berezinsky, A. Gazizov, S. Grigorieva, *Phys. Rev. D* **74** 043005 (2006).
- [59] R.U. Abbasi et al., *Phys. Rev. Lett.* **100** 101101 (2008).
- [60] S. Sarangi and S.-H. Tye, *Phys. Lett.* **B536**, 185 (2002).
- [61] E.J. Copeland, R.C. Myers and J. Polchinski, *JHEP* 0406, 013 (2004).
- [62] G. Dvali and A. Vilenkin, *JCAP* 0403, 010 (2004).